Physical Optics Analysis of the ALMA Band 5 Front End Optics

Mark Whale[1,*], Neil Trappe[1], and Victor Belitsky[2]

[1]*National University of Ireland, Maynooth, Co. Kildare, Ireland*

[2]*Group for Advanced Receiver Development, Chalmers Technical University, Gothenburg, Sweden*

- Contact: mark.r.whale@nuim.ie, phone +353-1-708 4668

***Abstract* — The Atacama Large Millimetre Array will be a ground based millimetre to submillimetre band interferometer. The instrument will be comprised of up to 50 high precision 12m Cassegrain antennas. Each antenna will cover a frequency range from 30 to 950 GHz, which will be split into 10 observing channels/bands. Each frequency channel will have its own specifically designed front end optics to couple radiation from the secondary reflector focal plane to the accompanying receiver. We present a full electromagnetic analysis of the band 5 front end optics system using physical optics, which covers a range from 163 to 211 GHz. This band is being developed by the Group for Advanced Receiver Development (GARD) at Chalmers University, Gothenburg, Sweden. Two software packages are utilised for this analysis; the industry standard reflector antenna software package GRASP9 developed by TICRA [1] and a new optical software package MODAL [2,3] (Maynooth Optical Design Analysis Laboratory) developed at NUI Maynooth, Ireland. Electromagnetic predictions of beam patterns are presented at the Cassegrain focal plane and at the subreflector vertex.**

The basis of the analysis is primarily to determine optical performance and efficiency and the effects of beam truncation by the off-axis reflectors of the front end optics. Three levels of beam truncation are modelled varying rim diameter.

I. Introduction

A. The ALMA Instrument

The Atacama Large Millimetre Array is an international project to construct a ground based interferometer array to work in the submillimetre/far-infrared region and is considered to be the successor to the present generation of millimetre and sub-millimetre wave interferometers. The ALMA instrument will utilise high resolution radio astronomy techniques applied to the millimetre/submillimetre region, allowing astronomers to observe the cool Universe, determine the chemical composition the molecular gas and dust in star forming regions, observe the redshifted dust continuum emission from galaxies at various epochs of evolution, reveal the kinematics of previously obscured Galactic Nuclei and Quasi-Stellar Objects and obtain high resolution images of cometary nuclei, asteroids and Kuiper Belt Objects along with the planets of the Solar System and their satellites [4].This research is carried out with our collaborators at the Group for Advanced Receiver Development (GARD), Chalmers Technical University, Gothenburg, Sweden.

The instrument will be comprised of 50 12m antennas with 25*um* surface accuracy and 0.6″ pointing precision. This array of antennas can be arranged into various configurations with maximum and minimum widths of 14km and 150m respectively. The array will be located 5000m above sea level on the Chajnantor plane in the Atacama region of Chile, which will provide excellent atmospheric transparency for the observable millimetre and sub-millimetre waveband [5].

B. The ALMA Front End Receivers

The ALMA instrument will have frequency coverage from 30GHz to 950 GHz in 10 dual polarisation bands. Each of these bands has a modular 'plug in' design, and all 10 bands are housed in a single dewar flask, located at the Cassegrain focal plane, meaning that all frequency bands share the same focal plane, removing any need for a selection mirror arrangement. The bands are divided into 3 separate categories; indicative of the requirements of the particular receiver frequency. Category A receivers (bands 1 & 2) contain 'warm' optics; Category B receivers contain a mixture of 'warm' and 'cold' optics (bands 3 & 4) and Category C receivers contain entirely 'cold' optics (bands 5 – 10) [6]. The work presented in this paper is devoted to the analysis of the band 5 receiver, a Category C receiver.

II. APPLICATION

A. ALMA Band 5 - Introduction

The design and assembly of this band is the responsibility of the Radio and Space Science Department at the Chalmers University of Technology in Gothenburg, Sweden. Quasioptical and physical optical analysis of this receiver has been conducted at NUI Maynooth. The ALMA band 5 receiver has a frequency range of 163GHz to 211 GHz with a central operating frequency of 187GHz. It is comprised of two off-axis ellipsoidal reflectors, which couple the Cassegrain focal plane to the circular corrugated receiver horn (c.f. figure 1). Dual polarisation is achieved in the band with an orthomode transducer at the back of the waveguide. The analysis presented in this paper includes a full quasioptical treatment of the system and physical optics software simulations, which include predictions of aperture efficiency, subreflector edge taper, *beam Gaussicity and cross* polar levels. Physical optics predictions are also used for a comparison of system efficiency against varying reflector rim diameters and to verify an improvement to system efficiency with a redesign of the ellipsoidal reflector geometries.

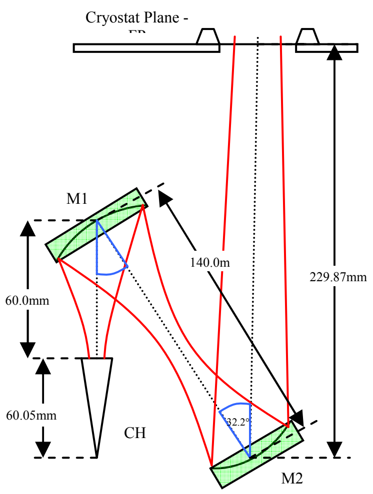

Fig. 1 ALMA band 5 front end optics layout

B. *ALMA Band 5 – Software Models*

The beam parameters for band 5 were obtained by propagating a fundamental Gaussian beam through an ABCD matrix representation of the system. Using ABCD matrices, the beam parameters can be calculated at any position throughout the system. Using these parameters and the diagram of the system layout, a model of the system was generated in the GRASP9 and MODAL packages.

1) *Ellipsoidal Reflectors:* The initial geometry of the ellipsoidal reflectors for the band 5 front end receivers was designed with geometrical optics. This was taken as a design practice throughout the ALMA receivers, which would make for easier optical verification. However, geometrical layouts are less efficient in the millimetre/submillimetre region. A reflector designed using geometrical optics will not correctly match the complex phase radius of curvature of the incident beam, and as such, optical aberrations will occur. As an improvement on the reflector design, 'Gaussian' optics was used, where the radius of curvature of the ellipsoidal reflector will match the input phase radius of curvature for the central frequency of 187GHz. A comparison between the standard geometrical optics and Gaussian optics is also presented. This comparison will reveal any losses in performance neglecting long wavelength effects.

2) *Circular Corrugated Horn*: The feed for the system is a circular corrugated horn, designed by the research group at Chalmers. Rather than using a fundamental Gaussian field or a truncated Bessel field as an approximation to the source field, a full waveguide multimoded aperture field is calculated and used as an input field. This aperture field was generated using a mode-matching scattering matrix software package that was developed at Maynooth called SCATTER. The near and far field descriptions calculated from SCATTER [7] have been verified against various experimental data. This aperture field is propagated through the system in GRASP9 as an external source object. The SCATTER code is part of the MODAL software and a simple geometry description of the horn is required to describe the input horn field.

3) *Reflector Rim Truncation*: As well as a geometrical and Gaussian optics design comparison, it was also necessary to perform physical optics analysis of the effect of the off-axis reflector rim truncation of the beam for varying mirror size. In designing any optical reflector system, conservation of power is important. One must strive to confine as much power as possible within the reflector area and reduce spillover. In this compact off-axis reflector system, analysis of this power conservation is more important since there are opto-mechanical limits to be considered. The best overall system is a compromise between the maximum power confined within the reflector area and the maximum allowable reflector size within the band 5 cartridge. For this analysis, 3 different rim radii were considered. These reflector rim radii are multiples of the lowest frequency beam waist at each reflector; $4.0w_{163}$, $4.5w_{163}$ and $5.0w_{163}$, each representing varying degrees of truncation of the incident beam. The lowest frequency waist was chosen since this represents the largest beam waist across the bandwidth, and is thus considered the upper limit of truncation. The results presented for both the geometrical and Gaussian optics versions are given for the upper, middle and lower frequencies and each of the 3 reflector rim radii.

III. RESULTS

From the physical optics simulations of the two versions of the band 5 system, beam pattern measurements were made at two locations; the focal plane which represents the cryostat plane and the subreflector vertex plane. Using these beam pattern measurements, several calculations were made determining the performance of the band 5 system in terms of aperture efficiency (coupling efficiency of the output beam to the sky), edge taper at the subreflector (the amount of power confined to within the subreflector area), Gaussicity (how well the output field couples to a fundamental Gaussian beam) and cross polarisation efficiency (how much power present in the cross polar field relative to the co polar field).

A. *Aperture Efficiency*

Antenna aperture efficiency is represented as the coupling efficiency between the beam at the subreflector vertex plane and a truncated plane wave.

$$\eta_a = \left| \frac{\int_{AP} E_a^* E_{tpw} \, dS}{\sqrt{\int_{AP} |E_a|^2 dS \int_{AP} |E_{tpw}|^2 dS}} \right|^2 \quad (1)$$

where *AP* represents an integral over the entire aperture plane, E_a is the aperture field and E_{tpw} is the ideal truncated plane wave field [8]. The truncated plane wave used here contains a scaled central blockage, to account for the degradation in the aperture efficiency from the central blockage shadowing of the secondary mirror over the primary reflector. As such, this aperture efficiency calculation takes into account the coupling efficiency, spillover efficiency and the blockage efficiency.

Non ideal smoothness of the mirror surfaces from their ideal shape introduces perturbations in the wavefront and thus leads to a decrease in the aperture efficiency. Studies conducted by Ruze [9] show that the actual mirror surface deformations can be statistically modeled assuming that phase errors of a surface point have a mean zero and belong to a Gaussian population of RMS deviation about this mean. Therefore, small-scale surface errors decrease the efficiency and are described by

$$\eta_{Ruze} = Exp\left(-16\pi^2 \frac{\left(\sigma_s^2 + \sigma_p^2\right)}{\lambda^2}\right) \qquad (2)$$

TABLE I
APERTURE EFFICIENCY COMPARISON

Rim	η	*Freq (GHz)*	Geom	Gauss	*Freq (GHz)*	Geom	Gauss	*Freq (GHz)*	Geom	Gauss
4.0*w*	η_a	163	0.829	0.845	187	0.841	0.855	211	0.851	0.861
	η_b		0.822	0.838		0.833	0.849		0.844	0.855
	η_r		0.934	0.934		0.924	0.924		0.915	0.915
	η_t		**0.768**	**0.783**		**0.770**	**0.784**		**0.772**	**0.782**
4.5*w*	η_a		0.836	0.860		0.845	0.863		0.853	0.865
	η_b		0.829	0.853		0.838	0.856		0.846	0.859
	η_r		0.934	0.934		0.924	0.924		0.915	0.915
	η_t		**0.774**	**0.797**		**0.774**	**0.791**		**0.774**	**0.786**
5.0*w*	η_a		0.836	0.865		0.846	0.866		0.852	0.870
	η_b		0.829	0.859		0.838	0.859		0.845	0.862
	η_r		0.934	0.934		0.924	0.924		0.915	0.915
	η_t		**0.774**	**0.802**		**0.774**	**0.794**		**0.773**	**0.789**

In the above table, η_a represents coupling efficiency to an unaltered truncated plane wave, η_b represents coupling efficiency to a truncated plane wave including the central blockage, η_r represents the Ruze factor using a value of 25 microns for surface accuracy [5], and η_t gives the total combined aperture efficiency.

The required ALMA standard aperture efficiency is for coupling of the output beam at the subreflector to the truncated plane wave field of > 80%. This is given by η_a and as can be seen from Table 1, this value is above the required 80% efficiency. Note the increase in aperture efficiency when we go from the geometrical design to the Gaussian design. This is a good validation of the advantages of Gaussian optics laws applied to the reflector design.

B. Subreflector Edge Taper

The edge taper at the subreflector is the relative power density within a specified radius *r*. In this case, the edge taper represents the amount of power confined within the subreflector, which has a radius of *375mm*. For a fundamental Gaussian beam, the edge taper T_e is given as:

$$T_e = Exp\left(-2\left(\frac{r}{w}\right)^2\right) \qquad (3)$$

where *r* is the radius of the beam r and *w* is the beam waist.

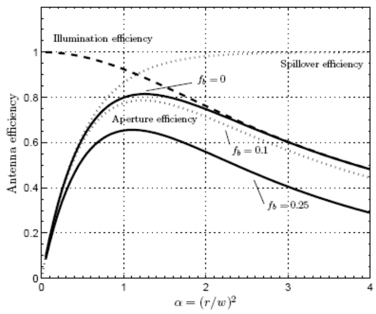

Fig. 1 Aperture efficiencies for a circular antenna with Gaussian illumination. The aperture efficiency η_a is the product of the illumination efficiency η_{ill} and the spillover efficiency η_s. [7]

The truncation of the equivalent fundamental Gaussian beam for the subreflector gives an edge taper of -12dB which optimizes the equivalent Truncated Bessel field representing a scalar horn input. However, the maximum aperture efficiency for an unblocked Gaussian illumination is -10.9dB [8] – c.f. figure 1.

TABLE II
SUBREFLECTOR EDGE TAPER COMPARISON

Freq (GHz)	Rim	T_e *(dB)* - Gauss	T_e *(dB)* - Geom
163	4.0*w*	-10.71	-11.34
	4.5*w*	-11.05	-11.29
	5.0*w*	-11.17	-11.42
187	4.0*w*	-11.25	-11.40
	4.5*w*	-11.52	-11.73
	5.0*w*	-11.55	-11.80
211	4.0*w*	-11.65	-11.45
	4.5*w*	-11.73	-11.43
	5.0*w*	-11.72	-11.42

From the results presented in table 2, it is clear that results from both designs of the band 5 system give very acceptable power conservation at the subreflector.

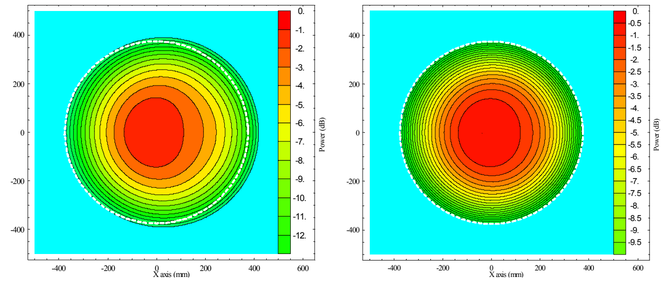

Fig. 2 Contour plots of the beam taken at the subreflector vertex plane illustrating the amount of power incident on the subreflector – the white circle indicates the position of the subreflector rim

The contour plots illustrated in figure 2 shows two contour plots of the beam at the subreflector vertex plane. Note the improved beam symmetry in the improved Gaussian optics design (right) over the geometrical optics design (left).

C. *Cross Polar Efficiency*

Cross polar efficiency is an important factor in off axis reflector systems. It has been shown that off axis paraboloids and ellipsoids increase the levels cross polar power, thus decreasing the amount power conserved to the co polar component [10]. However, for systems of compensating off axis reflectors, such as the band 5 system, any cross polar power created by one mirror should be removed, or 'compensate' for by the second. The levels of cross polar power were normalised against co polar power at the focal plane and the subreflector plane.

The design goals for the ALMA front end receivers require a maximum cross polar level of -25dB. Table 3 lists the cross polar levels as predicted by the mode matching software SCATTER for the corrugated horn aperture and table 4 lists the predicted cross polar levels from the band 5 system at the focal plane (FP) and the subreflector vertex (SUB) for both the geometrical and Gaussian optics designs.

TABLE III

CROSS POLAR EFFICIENCY COMPARISON

Freq (GHz)	163	187	211
XsP (dB)	-37.40	-36.43	-29.42

TABLE IV

CROSS POLAR EFFICIENCY COMPARISON

Freq (GHz)	Rim	*XsP (dB)* - Gauss		*XsP(dB)* - Geom	
		FP	*SUB*	*FP*	*SUB*
163	4.0w	-31.13	-31.46	-31.05	-31.31
	4.5w	-30.96	-31.19	-30.97	-31.05
	5.0w	-30.83	-31.04	-30.85	-30.89
187	4.0w	-32.28	-32.54	-32.17	-32.47
	4.5w	-32.09	-32.43	-32.21	-32.32
	5.0w	-32.01	-32.35	-32.13	-32.21
211	4.0w	-29.17	-29.23	-29.19	-29.30
	4.5w	-29.07	-29.16	-29.12	-29.19
	5.0w	-29.02	-29.10	-29.07	-29.11

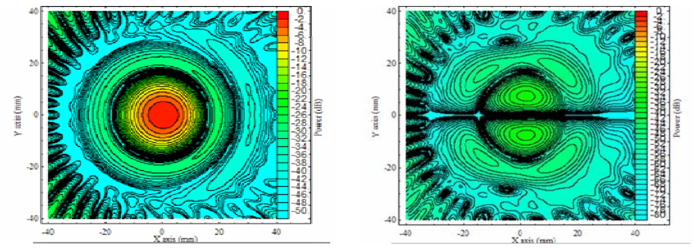

Fig. 3 Co polar (left) and cross polar (right) beam pattern plots at the focal plane for the central frequency (187GHz) for the Gaussian optics version of band 5

From the above tables it can be seen that the band 5 system is very efficient at maintaining the low levels of cross polar power from the circular corrugated horn aperture. For all rim truncations and for both geometrical and Gaussian optics designs, the cross polar levels do not rise above -25dB.

The contour plots above in figure 3 give an example of the copolar and cross polar beams at the band 5 focal plane.

D. *Performance of MODAL Software Package*

Throughout the analysis of the band 5 system, GRASP9 was considered as the benchmark optical software package for Physical Optics beam calculations. The same analysis was performed using the MODAL optics software package as both a further reliability test to the abilities of the package and a validation of the band 5 system. The performance of the MODAL package has been demonstrated in previous papers [2,3]. The beam pattern predictions by MODAL were compared against those from GRASP9 using a coupling integral, similar to calculating aperture efficiency. This coupling revealed an average coupling of 99.6% for copolar beams and 97.8% for cross polar beams. These results are an excellent validation for the performance of the MODAL optics software package.

CONCLUSIONS

Overall the electromagnetic predictions of the band 5 system have performed as expected. Since the band 5 system is awaiting construction, comparisons of electromagnetic predictions against experimental values are planned. The effect of varying rim diameters on the beam has been predicted, and the improvement in system performance with a Gaussian design of the reflector surfaces has been shown. With the Gaussian optics design of the system, we have seen an improvement in the aperture efficiency levels and an improved symmetrical focusing of the beam on the subreflector. With an increase in rim size for both versions of the system we have seen improved aperture efficiency levels, which is to be expected since an increase in collecting area leads to an increase in conserved power between the aperture and the feed. Cross polar efficiency for both versions is excellent, with levels at the subreflector matching the levels at the horn aperture.

The results presented in this paper have been taken into consideration by the GARD group for their planned design of the band 5 system. It has been decided that the Gaussian optics design will be used over the geometrical design and a rim truncation of 5.0*w* will be implemented. This will give the best possible performance from the system as predicted by the analysis presented here.

ACKNOWLEDGMENT

We would like to thank NUI Maynooth, Enterprise Ireland and Science Foundation Ireland for supporting this work financially. We would also like to thank the GARD group at Chalmers Technical University.

REFERENCES

[1] GRASP9 – General Reflector and Antenna Farm Analysis Software, TICRA, Læderstræde, Copenhagen, Sweden

[2] M.L Gradziel, D. White, S. Withington, J.A. Murphy, "*Fast CAD Software for the Optical Design of Long Wavelength Systems*" 2005 Joint 30th Intl. Conf. On Infrared and Millimetre Waves

[3] O'Sullivan, C. J.A. Murphy, G. Cahill, M.L. Gradziel, N. Trappe, D.White, V. Yurchenko, S. Withington, W. Jellema, "Developments in Quasi-Optical Design for THz," Proc. SPIE-04, Glasgow, UK, 21-25 June 2004, #5498-39, June 21-25, 2004.

[4] (2002)"*Science with ALMA*", ESO website document [Online] Available at http://www.eso.org/projects/alma/science/alma-science.pdf

[5] (2002) The ALMA project book website [online] Available at http://www.alma.nrao.edu/projectbk/construction/

[6] Rudolf, M. Carter, A. Baryshev, "The ALMA Front End Optics – System Aspects and European Measurement Results", IEEE Trans. on Antennas and Propagation, Vol. 55, No. 11, November 2007

[7] Gleeson, "Single and multi-moded corrugated horn design for cosmic microwave background experiments", PhD thesis, NUI Maynooth, Co. Kildare, Ireland, 2004

[8] P.F. Goldsmith, "Quasioptical Systems: Gaussian Beam Quasioptical Propagation and Applications", IEEE Press, Wiley Publishers.

[9] Ruze, "Antenna Tolerance Theory – A Review" Proc. IEEE, Vol. 54 p.633-640, April 1966

[10] J.A. Murphy, S. Withington, "Perturbation Analysis of Gaussian Beam Mode Scattering at Off-Axis Ellipsoidal Mirrors", Infrared Physics & Technology, Issue 37, 1996, p 205-209.

.